CHAPTER 3

METHODOLOGY

In this chapter, the research procedure is described in details i.e. the x-ray absorption spectrum measurement, x-ray absorption edge identification of atomic oxidation state of absorbing atom, x-ray absorption near edge structure verification of local structure geometry around absorbing atom and extend x-ray absorption fine structure extraction of local structure information around absorbing atom.

3.1 Research procedure

In this research, the local structures of doped and undoped perovskite oxide compounds were investigated using x-ray absorption spectroscopy (XAS). The x-ray absorption spectra of absorbing atom in the samples and their standards were measured at Beamline 8, Siam Photon Laboratory, Synchrotron Light Research Institute (SLRI). The software package based on IFEFFIT library [15, 16] equipped with numerical and analytical algorithms was used to optimize and analyze the x-ray absorption spectra. In this software package, there consists of several programs for the x-ray absorption spectra analysis. The program ATHENA was used to optimize x-ray absorption spectra. The x-ray absorption spectra were normalized during the XANES analysis, and converted to either *k*-space or *r*-space in the EXAFS analysis. Then, the program ATHENA was used to analyze the XANES spectra. After normalization, the XANES spectra at the absorption edge position of the samples were compared with their standards to identify the oxidation state of absorbing atom. This knowledge of the oxidation state can be used to predict the atomic environment around absorbing atom. To further verify the predicted position of absorbing atom in the samples, the program ATOMS was used to generate atomic position of model structure. After that, with the supplied model structure information, the program FEFF was used to compute x-ray absorption spectra based on ab initio self-consistent multiple-scattering calculations. The comparison between the measured and calculated XANES spectra was used to confirm the atomic position of absorbing atom in the samples. Then, the program

ARTEMIS was used to analyze EXAFS spectra. The converted EXAFS spectra in both *k*-space and *r*-space were least square fit with scattering paths to model the experimental spectra, while using program FEFF to compute the scattering parameters. The purpose of the fitting is to extract the local structure information around absorbing atom. The research procedure is shown in Figure 3.1.

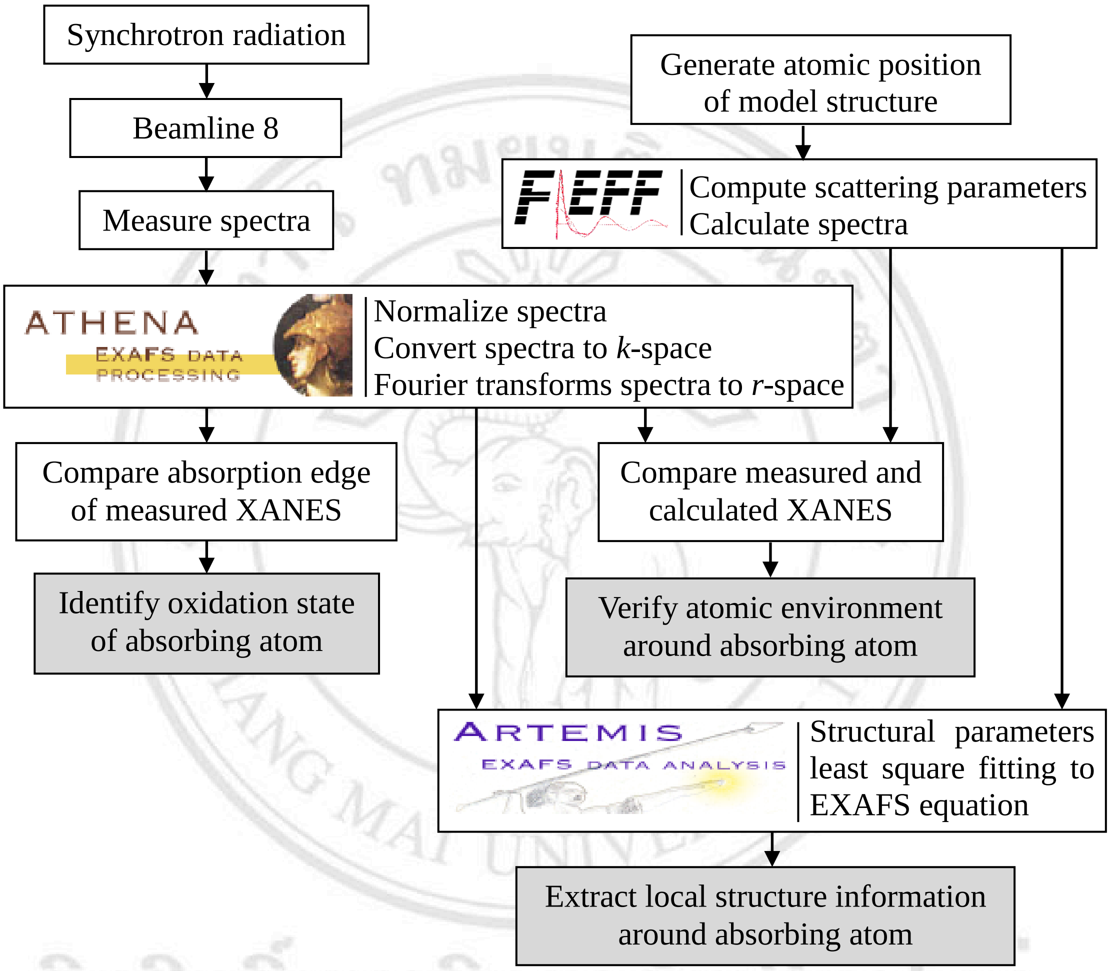

Figure 3.1 The research procedure.

3.2 X-ray absorption spectrum measurement

The x-ray absorption spectra of absorbing atoms in the sample and its standards were measured at Beamline 8, Siam Photon Laboratory, Synchrotron Light Research Institute (SLRI). Synchrotron is the complex machines built for high energy physics experiments. It is used to accelerate charged particles up to relativistic speeds, i.e. the particle velocity v approaches the speed of light c. The electrons are usually used in synchrotron which can be generated from the cathode tube. Linear accelerator increases the kinetic energy of the beam by passing groups of electrons through conducting cavities in which a radio frequency electromagnetic standing wave is maintained. Booster synchrotrons accelerate the electrons up to the desired energy (1.0 GeV), after which they are transferred to "storage ring" under ultrahigh vacuum (10^{-10} torr). In storage ring, a radio frequency electromagnetic standing wave accelerates the electrons to higher energy (1.2 GeV). The accelerating charged particles generate electromagnetic radiation when traveling through bending magnets in storage ring. Synchrotron radiation extends over a broad energy ranges from infrared to x-ray as shown in Figure 3.2.

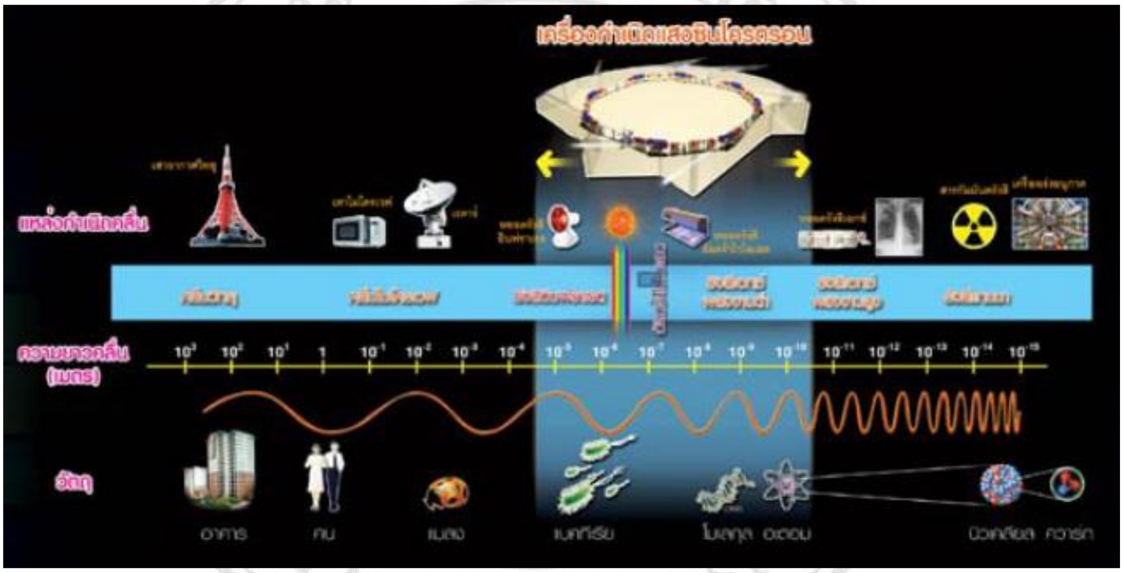

Figure 3.2 The wavelength of electromagnetic that generate from synchrotron radiation [17].

Synchrotron radiation yields continuous x-ray energies with high intensity as shown in Figure 3.3. It can be used to study x-ray absorption spectroscopy. In SLRI, the synchrotron radiation source can generate x-ray energy ranges from about 1.25 keV to 10 keV covering the absorption edges of most atoms: *K*-edge absorption for atomic number from 11 to 31, *L*-edge absorption for atomic number from 32 to 70 and *M*-edge absorption for atomic number from 71 to 92.

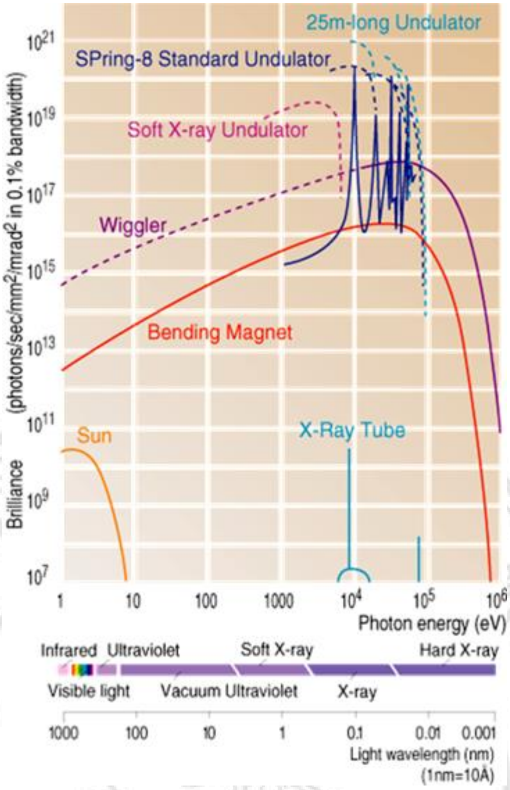

Figure 3.3 The brilliance of x-ray photon generate from several sources [18].

In order to measure x-ray absorption spectroscopy of an absorbing atom in the sample, the white synchrotron beam, the source of x-ray energies source, need to be increased the pressure from ultrahigh vacuum (10^{-10} torr) in the storage ring to high vacuum (10^{-7} torr) in the pressure reduction tube (PRT). In this tube, the vertical and horizontal apertures are used to control the beam size before entering the x-ray absorption spectroscopy experimental station. The typical experimental arrangement for x-ray absorption spectroscopy measurement is shown in Figure 3.4.

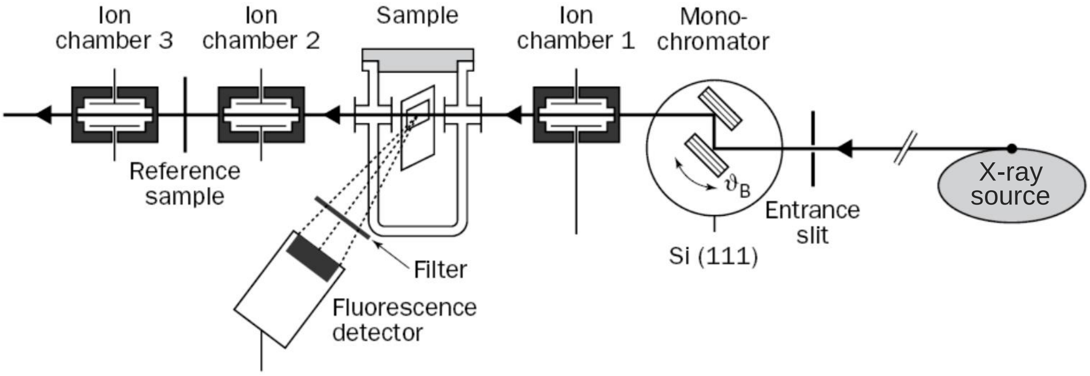

Figure 3.4 The typical set-up for measuring x-ray absorption spectroscopy in transmission and fluorescence modes [11].

In the x-ray absorption spectroscopy experimental station, the white synchrotron beam is resized by the entrance slit which matches to that of the sample size. The position and size of the white synchrotron beam can be observed from x-ray beam position monitor (XBPM). After that, the double crystal monochomator (DCM) is used to select the desired energy of the white synchrotron beam, based on Bragg's law [19] i.e.

$$2d\sin\theta_{\mathrm{B}} = n\lambda, \tag{3.1}$$

where d is the distance between the planes in atomic lattice, θ_{B} is the incident x-ray angle, n is the diffraction order (commonly equal to 1) and λ is the incident x-ray wavelength (i.e. $\lambda = hc/E$, where h is Planck constant, c is the speed of light in vacuum and E is the incident x-ray energy). The most important component of the double crystal monochomator is the parallel symmetric-cut crystals (with crystal surface parallel to lattice plane). When the white synchrotron beam with several energy shines upon the first crystal, only the x-ray that satisfy Bragg's law are diffracted and the monochromatic x-ray is emitted. After that, the monochromatic x-ray is reflected by the second crystal in the direction parallel to that of the incoming white x-ray as shown in Figure 3.5.

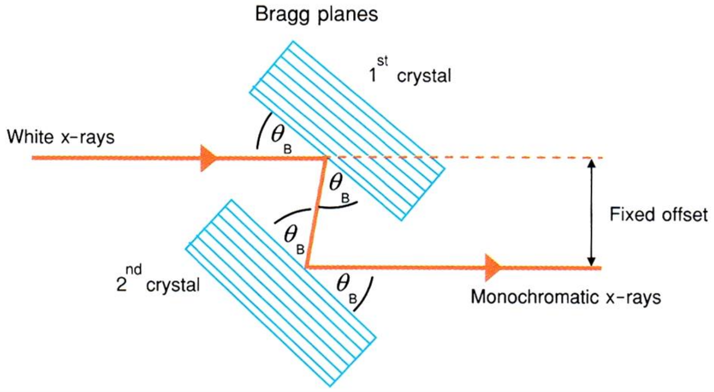

Figure 3.5 The rotating double crystals used to select the x-ray energy [20].

The energy of the x-ray that passes the double crystal monochromator is varied by rotating the double crystal that the white beam shines on. However, in BL8, the double crystal monochomator can be rotated from 13.7° to 65°. Therefore, several kinds of double crystals (different lattice spacing *d*) have to be used to measure the x-ray absorption of most absorbing atom as shown in Table 3.1.

Table 3.1 Double crystals and their corresponding photon energy ranges used in the double crystal monochromator [20].

Double crystal	2*d* Spacing (Å)	Photon energy ranges (eV)
KTP(011)	10.955	1,250 - 4,780
InSb(111)	7.481	1,830 - 7,000
Si(111)	6.271	2,180 - 8,350
Ge(220)	4.001	3,440 - 13,000

In the double crystals monochomator, the pressure is increased to 10^{-5} torr. The Kapton window (tiny absorbed x-ray) is used to separate the rough vacuum in the absorption coefficient measurement section. In this BL8, there are two modes to measure the absorption coefficient of an absorbing atom i.e. the transmission mode which is good for thin and concentrated ($>$ 5%wt) sample and fluorescence mode which is good for think and diluted ($\leq$ 5%wt) sample.

Transmission mode is the most straightforward; it simply involves measuring the x-ray flux before and after the beam is passed through a homogeneous sample. Under these conditions, the incident flux I_0 and the transmitted flux I are measured in ionization chambers to calculate the absorption coefficient of the sample (and its reference) according to Lambert-Beer’s law (Eq. 2.1). Therefore, the sample is placed at 90° to the incident beam and the ionization chambers in the horizontal plane. In the ionization chamber, a parallel plate capacitor is filled with the different gases (1 bar), where high voltage (300 V/cm) is applied across (in the direction perpendicular to the x-ray beam direction) as shown in Figure 3.6. When x-ray beam passes through the ionization chamber, the gases inside will be immediately ionized and travel to the opposite charge electrodes. The x-ray flux can then be calculated from the electric current.

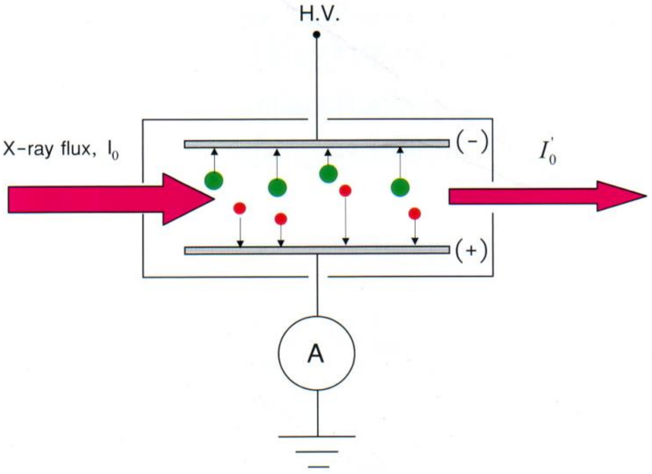

Figure 3.6 The ionization chamber [20].

In x-ray flux measurement, the ionization chambers have a length of 10 cm and 40 cm are used to measure the incident flux and transmitted flux, respectively. These ionization chambers are filled such that the absorption level in the first ionization chamber is 10%, in the second ionization chamber 90% as shown in Table 3.2. Since the gases and the pressure in the ionization chambers depend on the energy of the absorption edge.

In the fluorescence mode, one measures the incident intensity I_0 and the fluorescence x-ray intensity I_f that are emitted in following the x-ray absorption event. Several kinds of fluorescence detectors (e.g. Lytle detector, Si detector and 13 element Ge detectors) are used to measures the fluorescence x-ray. Usually, the fluorescence detector is placed at 90° to the incident beam in the horizontal plane, with the sample at an angle (usually 45°) with respect to the beam. The absorption coefficient is therefore calculated from I_0 and I_f ratio.

Table 3.2 The appropriate gases pressure filled in the ionization chambers for x-ray absorption spectroscopy measuring various absorption edges of absorbing atoms [20].

K-edge	L_3-edge	M_5-edge	Ion chamber 1	Ion chamber 2
Mg	As, Se		N_2 6 mbar	N_2 31 mbar
Al	Br, Kr	Ta, W	N_2 10 mbar	N_2 53 mbar
Si	Rb, Sr	Re, Os	N_2 16 mbar	N_2 85 mbar
P	Y, Zr	Ir, Pt, Au, Hg	N_2 24 mbar	N_2 132 mbar
S	Nb, Mo	Tl, Pb, Bi, Po	N_2 37 mbar	N_2 200 mbar
Cl	Tc, Ru	Po, At, Rn, Fr	N_2 54 mbar	N_2 296 mbar
Ar	Rh, Pd, Ag	Ra, Ac, Th, Pa	N_2 79 mbar	N_2 433 mbar
K	Cd, In	U	N_2 113 mbar	N_2 619 mbar
Ca	Sn, Sb, Te		N_2 160 mbar	N_2 872 mbar
Sc	I, Xe		Ar 11 mbar	Ar 61 mbar
Ti	Cs, Ba		Ar 15 mbar	Ar 80 mbar
V	La, Ce		Ar 19 mbar	Ar 104 mbar
Cr	Pr, Nd		Ar 24 mbar	Ar 133 mbar
Mn	Pm, Sm		Ar 31 mbar	Ar 170 mbar
Fe	Eu, Gd, Tb		Ar 39 mbar	Ar 214 mbar
Co	Dy, Ho		Ar 49 mbar	Ar 269 mbar
Ni	Er, Tm		Ar 61 mbar	Ar 335 mbar
Cu	Yb, Lu		Ar 76 mbar	Ar 413 mbar
Zn	Hf, Ta, W		Ar 93 mbar	Ar 509 mbar

At the beginning of the measurement, it is common to measure the absorption of a pure material along with the sample as a reference to calibrate the motor of double crystal monochomator offset. A short period complete spectrum is measured and one can easily decide whether the measurement conditions, such as energy range or sample position, need to be changed. This way, only a minimum amount of beamtime is lost if the spectrum needs to be optimized by changing some parameters.

3.3 Data processing with ATHENA

Practically, the x-ray absorption spectra measured from experimental require noise reduction to avoid errors in the extensive analysis results. In order to increase the signal-to-noise ratio, the multiple spectra, e.g. taken from different samples, should be collected. The spectra need to be aligned to the same absorption edge energy. To align the spectra, the absorption edge energy of one spectrum relative to one another has to be shifted until both spectra match. After multiple spectra are aligned in this way, they can be merged into one spectrum. Then, the calibration for the absolute absorption edge energy has to be performed. Since the absorption edge energy of the reference spectrum corresponds to the standard tabulated absorption edge energy [7] and can be used to define the absolute absorption edge energy. To calibrate the absorption edge energy, the absorption edge energy of the reference spectrum has to be defined. Since the absorption edge usually has a non-negligible width, the choice of the absorption edge energy is arbitrary and different definitions can be used. Generally, the maximum of the first peak of the first derivative of the spectrum is defined as the absorption edge energy. To calibrate spectrum, the absorption edge energy of the reference spectrum is shifted in such a way that the maximum of the first peak of the first derivative coincides with the tabulated edge energy. The same energy shift procedure, in the final calibration step, also applies to the average spectrum of the sample.

In order to compare the x-ray absorption spectra measured from different samples, the spectra have to be normalized. The variations in the height of absorption edge could be resulted from the different concentrations of absorbing atoms, sample thickness or detector settings. Therefore, the absorption edge step $\Delta\mu_0(E)$ should be normalized to one and the absorption pre-edge region $(E < E_0)$ should be set to zero (see Figure 3.7). The normalization is accomplished by fitting a line to the pre-edge region $(E < E_0)$ and the post-edge region $(E > E_0)$ and extrapolates it over the whole spectrum energy ranges. The fit is controlled by the order of polynomial with degree ranges from 1 to 3 depending on the x-ray absorption spectrum. In normalization, the spectrum is subtracted by the pre-edge line and divided by the difference between the pre-edge line and the post-edge line $\Delta\mu_0(E)$ at the absorption edge energy E_0.

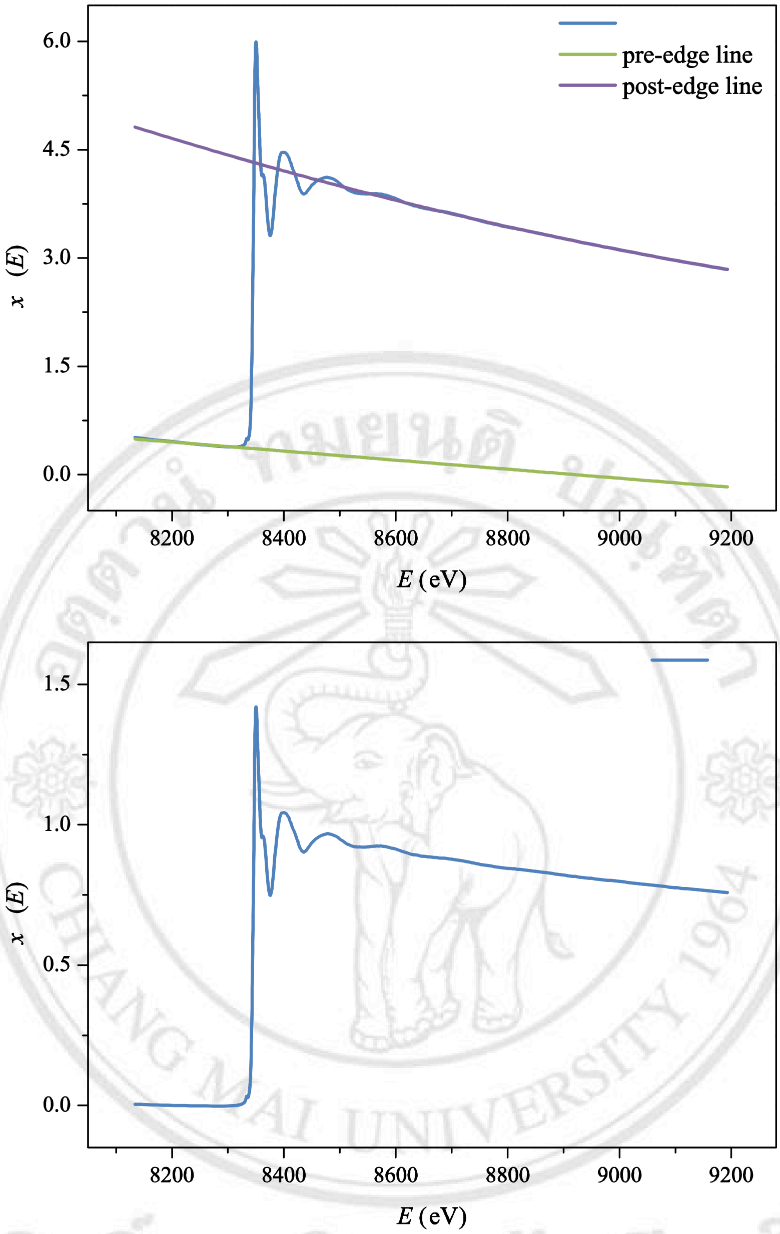

Figure 3.7 On the top panel, absorption pre-edge subtraction, used as the normalization, can be defined by the following. First, a pre-edge line (with a simple polynomial assumption) is fitted to the spectrum below the absorption edge. After that, the absorption edge step is estimated, and the spectrum is normalized using this value. The resulting normalized spectrum is shown in the bottom panel.

The most important step in the optimization of x-ray absorption spectrum is to subtract the background from the spectrum. The EXAFS is the oscillatory part of the absorption spectrum above the absorption edge, according to Eq. 2, becomes more prominent. The term $\mu_0(E)$ is the background function and is the absorption of an atom without neighboring interference. Unfortunately the background function is usually unknown and one cannot measure or calculate. One way to determine the background function is to do a spline fit. This spline fit could be a polynomial which might be of linear, quadratic or higher order. Different ways exist to place the knots (data for the fit) through the EXAFS oscillations. In early works the knots have been placed manually to optimize the background function. However, in this work, the AUTOBK approach (embedded in the program ATHENA [15, 16]) will be used to determine the background function [21]. In this approach, the knots are evenly spaced in photoelectron wave number. Then, the number of splines determines the maximum frequency component that is allowed in the background function. For instance, the number of cubic splines is given by

$$\text{the number of splines} = \frac{2R_{bkg}\Delta k}{\pi}, \qquad (3.2)$$

which the number of splines depends on the data range Δk and the number R_{bkg}. The number R_{bkg} has to be selected carefully and is usually chosen to be about one half of the nearest neighbor distance. The background function is then subtracted from the data (see Figure 3.8). After that, EXAFS oscillation as a function of energy, i.e. $\chi(E)$, is converted as a function of wave number, i.e. $\chi(k)$.

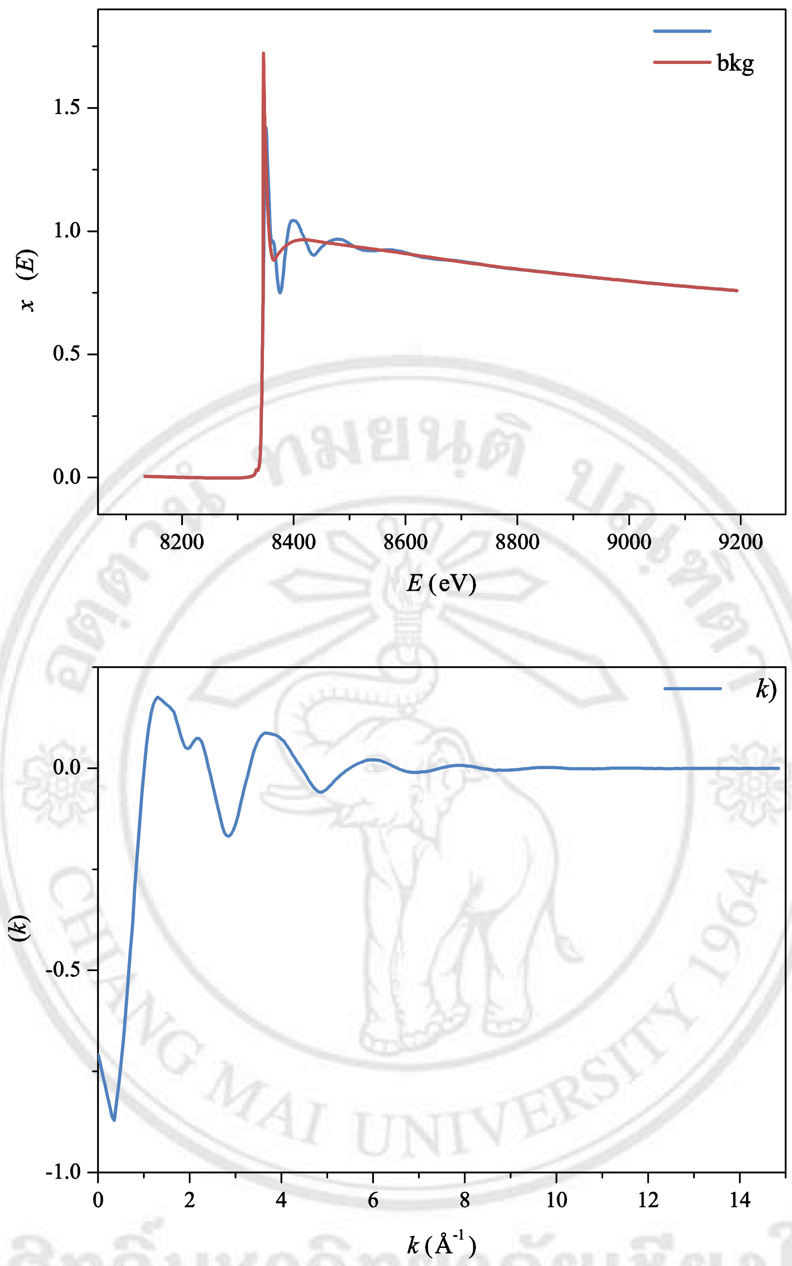

Figure 3.8 Comparison of the spline background function and the original $\mu(E)$ (top) and the post-edge background subtraction $\chi(E)$ converted to $\chi(k)$ (bottom).

In the analysis of EXAFS spectra, one possibility is to calculate theoretical spectra from model structures and fit these calculated spectra to the data to obtain the structural parameters of interest. The fitting can be done either in *k*-space or in the Fourier transformed *r*-space, where both the imaginary and the real parts of the Fourier transform are used. The inverse Fourier transform of $\chi(r)$ is again a function of wave number *k* (Eq. (2.14)). Different types of windows functions can be used to process EXAFS data. In this work the Hanning function will be applied as shown in Figure 3.9.

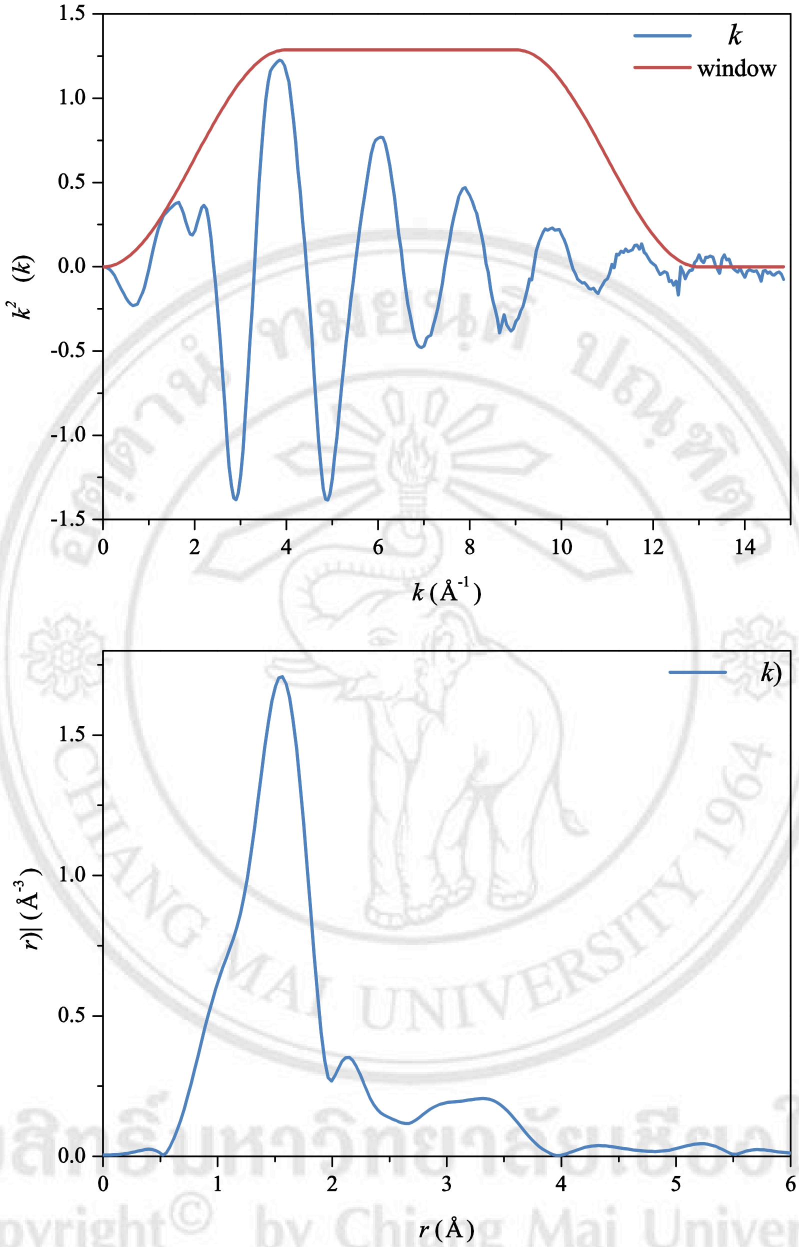

Figure 3.9 The EXAFS oscillations $k^2\chi(k)$ with Hanning window function (top) and its Fourier transform $\chi(r)$ (bottom).

After that, XAS spectrum is analyzed in both XANES and EXAFS regions using a software package for analyzing the XAS data. This package is based on the IFEFFIT library of analytical and numerical algorithms. The two main components are ATHENA, a program for XAS data analysis, and ARTEMIS, a program for EXAFS data analysis using theoretical standards from FEFF. These programs provide high quality analytical capabilities, can be run on all major platforms, and are freely available under the terms of a free software license.

3.4 The absorption edge analysis with ATHENA

In order to identify the oxidation state of absorbing atom in the investigated material, the absorption edge was analyzed with program ATHENA. Normally, an important and common application of the XANES is to use the shift of the absorption edge position to determine the oxidation state. The program ATHENA can be used to compare the absorption edge position of the sample and its standards with several oxidation states. The corresponding positions of the absorption edges can also be reliably used to empirically determine oxidation state. For the good x-ray absorption spectra, the oxidation state ratio can be determined with very good precision and reliability.

3.5 XANES analysis with ATHENA and FEFF

In order to identify the atomic environment around an absorbing atom in the investigated material, XANES analysis is discussed as following:

1. The predict position of absorbing atom in the model structure, which should resemble the structure of the investigated material as closely as possible, are generated using program ATOMS.

2. The simulated XANES spectra based on the prediction atomic environment around absorbing atom, are computed using program FEFF, which is based on ab initio self-consistent multiple scattering calculations [22]. Therefore, the absorbing atom environment can be indicated from the fingerprinting comparison of the simulated XANES spectra and the measured XANES spectra.

3.6 EXAFS analysis with ARTEMIS and FEFF

In order to extract the local structure information around absorbing atom in the investigated material, EXAFS analysis is based on the least squares refinement of scattering paths to model the experimental spectrum, was used in this work. This is as, from the EXAFS equation (see Eq. (2.13)), the distances between neighboring atoms *R*, the number of nearest neighbors N, the type of atoms in the different coordination shells Z and the mean square displacements of the atomic distances σ^2 can be determined as following:

1. The radial distribution of neighboring atoms around absorbing atom in the model structure, which should resemble the structure of the investigated material as closely as possible, are generated using program ATOMS (also embedded in the program ARTEMIS).

2. All possible scattering paths of the model structure are determined using the program FEFF (also embedded in the program ARTEMIS). For each scattering path, the effective scattering path length R_{eff} is calculated and the backscattering amplitude $F(k)$, the phase shifts $\delta(k)$ and the electron mean free path $\lambda(k)$ are stored for each path individually. The effective scattering path length R_{eff} is defined from half of distance that the photoelectron travels before returning to the absorbing atom. These parameters are calculated using the program FEFF, which is based on ab initio self-consistent multiple scattering calculations [22].

3. The model EXAFS equation, which construct from the sum of possible scattering paths of photoelectron scattered from neighboring atoms (see Eq. (2.13)), is fitted to the measured EXAFS spectrum using the program ARTEMIS [15, 16]. For each scattering path, which is selected and included in the fit, at least four parameters have to be defined, i.e. the change in the effective path length ΔR, the mean square displacement factor σ^2, the amplitude reduction NS_0^2 and the energy shift ΔE_0. The change in the effective path length ΔR is defined with respect to only the change in the half of total path length (the effective path length), e.g. for single scattering paths the distance between the absorber and the back scatter equals half the path length. The energy shift ΔE_0 accounts for any misalignment of the energy scale in the FEFF calculation with respect to the data. This misalignment is caused by the muffin-tin approximation, which is used to calculate the potential of the atoms [22]. The amplitude reduction term S_0^2 and the path degeneracy N correlate and might therefore considered as one parameter. The reduction term S_0^2 and the energy shift ΔE_0 apply for all paths

with one absorption edge, while the number of equivalent routes N depends on only one scattering path.

4. The scattering paths can be added in the fit while maintain the condition of the number of structural parameter N_{par} is less than that of independent point N_{idp} (see Eq. (2.15)). From the sum over scattering paths in the model EXAFS equation, the predicted structural parameters are optimized and accepted when the EXAFS from modeled equation corresponding to that of measured spectrum (R-factor is smaller than 0.02).

3.7 DFT calculation with ABINIT and QUANTUM ESPRESSO

In order to relax the distortion structure, DFT analysis is based on Kohn-Sham equation, was be used in this work

1. The predict position of absorbing atom in the model structure with lattice parameters was generated, which should resemble the structure of the investigated material as closely as possible.

2. The input parameter i.e. the plane wave cut off energy E_{cut}, the number of k-points, the pseudo-potential, and the type of exchange correlation energy approximation, were optimized in computational precision. The optimized input parameters related to quality of the calculation.

3. In the relaxation, each atom moves to the new position which minimizes the electric force and energy applying on the atom. The total energy is assumed to converge when the difference in total energies between the successive calculations is less than 10^{-5} eV.